Review of Experimental Modelling in Vascular Access for Hemodialysis

Drost, S.; Alam, N.; Houston, J. G.; Newport, D.

Published in:
Cardiovascular Engineering and Technology

DOI:
10.1007/s13239-017-0311-4

Publication date:
2017

Document Version
Peer reviewed version

Noname manuscript No.
(will be inserted by the editor)

Review of experimental modelling in vascular access for hemodialysis

S. Drost · N. Alam · J. G. Houston · D. Newport

Received: date / Accepted: date

Abstract This paper reviews applications of experimental modelling in vascular access for hemodialysis. Different techniques that are used in in-vitro experiments are bulk pressure and flow rate measurements, Laser Doppler Velocimetry (LDV) and Vector Doppler Ultrasound (VDUS) point velocity measurements, and whole-field measurements such as Particle Image Velocimetry (PIV), Ultrasound Imaging Velocimetry (UIV), Colour Doppler Ultrasound (CDUS), and Planar Laser Induced Fluorescence (PLIF). Of these methods, the ultrasound techniques can also be used in-vivo, to provide realistic boundary conditions to in-vitro experiments or numerical simulations. In the reviewed work, experimental modelling is mainly used to support computational models, but also in some cases as a tool on its own. It is concluded that, to further advance the utility of computational modelling in vascular access research, a rigorous verification and validation procedure should be adopted. Experimental modelling can play an important role in both in-vitro

S. Drost
Bernal Institute
School of Engineering
University of Limerick
Ireland

N. Alam
Bernal Institute
School of Engineering
University of Limerick
Ireland

J. G. Houston
Clinical Imaging and Image Guided Intervention
School of Medicine
Ninewells Hospital and Medical School
Dundee

D. Newport
Bernal Institute
School of Engineering
University of Limerick
Ireland E-mail: david.newport@ul.ie

validation, and the quantification of the accuracy, uncertainty, and reproducibility of in-vivo measurement methods.

Keywords Vascular Access · In-Vitro Experiments · Hemodialysis · Experimental validation · Hemodynamics

1 Introduction

In recent years, much research effort has been put into increasing the understanding of the relation between disturbed hemodynamics and the failure of different modalities for vascular access for hemodialysis. Several research groups and consortia worldwide (e.g. the European Union funded projects ARCH [40] and ReDVA [41]) work on clarifying the role of wall shear stress in vascular access non-maturation and stenosis. The ultimate goal of this work is to derive guidelines that can be used in the clinical practice, to improve the patency of Arterio-Venous Fistulas (AVF), Arterio-Venous Grafts (AVG), and Central Venous Catheters (CVC).

Important causes for vascular access failure are intimal hyperplasia and inadequate vascular remodelling [13,33]. Even though the understanding of the exact mechanisms behind these phenomena is still far from complete, it is widely accepted by now that hemodynamic wall shear stress plays an important role in this regard (see e.g. [5,13,33]). The creation of a vascular access site results in disturbed hemodynamics, which in turn leads to abnormal wall shear stress patterns. Disturbed wall shear stress can damage the endothelial layer of the blood vessel wall, and lead to intimal hyperplasia, stenosis, and ultimately thrombosis. As stenosis tends to develop at specific sites, it is expected that the geometry of the vascular access site, and the ensuing hemodynamics play a role. Therefore, much of the research in this field is aimed at developing computational models to study how parameters like vessel and graft geometry influence wall shear stress, and how to predict failure from quantities that can be measured in a clinical setting. Computational models allow for a detailed study of the local hemodynamics, with high spatial and temporal resolution.

In the end, these computational models are to be validated by clinical trials (see e.g. Caroli et al. [9]), by quantitatively comparing parameter values that can be measured in a clinical setting, such as flow rate. Often, as an intermediate step, experimental modelling is used. Although also experiments with test animals can be considered as experimental modelling, the scope of this paper is limited to experiments using in-vitro, bench-top set-ups. The main advantage of such set-ups is that they allow for highly controllable and reproducible experiments, which can be used to validate results from a computational model. However, once the simulation results are validated, the validity of the modelling assumptions should still be tested in-vivo.

Different definitions for verification and validation exist, and the terms are often used interchangeably. In the context of computational fluid dynamics, useful definitions are given by Oberkampf et al. [30], who use the term verification for the process of ascertaining that the discretised equations converge to the original analytical model equations (e.g. discretisation error estimation, mesh convergence), while the term validation is used to indicate testing whether the model, with all its assumptions, realistically represents the modelled process, within the intended range of parameter values.

The goal of this review paper is to give an overview of different approaches used in experimental modelling, their main results, and their suitability for particular applications. We briefly review the experimental methods used in in-vitro vascular access set-ups, and then move on to summarising the main results of studies using experimental modelling, grouped by vascular access modality. The review is concluded with a discussion to put the results into perspective, and recommendations for future work.

2 Background

2.1 Experimental techniques

The techniques used in experimental modelling in vascular access can be roughly classified as measurement of bulk parameters, like pressure and flow rate, point measurements, like Laser Doppler Velocimetry (LDV) and Vector Doppler Ultrasound (VDUS), and whole-field measurements, such as Particle Image Velocimetry (PIV), Ultrasound Imaging Velocimetry (UIV), Planar Laser Induced Fluorescence (PLIF), and Colour Doppler Ultrasound (CDUS). A brief overview of these techniques is given in table 1.

Table 1 Measurement techniques used in in-vitro hemodynamics experiments, with typical properties (* ultrasound vector and colour Doppler measurements can, in principle, be instantaneous, but usually some degree of averaging is applied to reduce noise and improve accuracy).

Method	**Principle**	**Quantity**	**Measurement type**
pressure sensor [37,17,18,4,6,39,38,11,10,26]	various	pressure	bulk, instantaneous, $\geq$ kHz
flow sensor [35,37,17,18,6,39,38,11,10,26]	various	flow rate	bulk, instantaneous, $\geq$ kHz
LDV [35]	optical	velocity	point, instantaneous, $\geq$ kHz
VDUS [22,21]	acoustic	velocity	point, average*, $\mathcal{O}(10)$ Hz
PIV [4,19,12,2,27,15,28,3]	optical	velocity	grid of points, instantaneous, $\mathcal{O}(10)$ Hz
UIV [20]	acoustic	velocity	grid of points, instantaneous, $\mathcal{O}(10-1000)$ Hz
PLIF [3]	optical	concentration	2D plane, instantaneous, $\mathcal{O}(10)$ Hz
CDUS [22,21]	acoustic	velocity	2D plane, average*, $\mathcal{O}(10)$ Hz

Different methods exist to measure bulk pressure and flow rate, including Pitot tube-type and piezo-electric pressure sensors, and paddle wheel or ultrasound-based flow rate sensors (for more information, see e.g. [36]). Point velocity measurements such as LDV and VDUS are based on the Doppler frequency shift induced by a moving reflector, for example, a particle or red blood cell carried along by a fluid flow [36,8,14]. Instantaneous whole-field velocity measurements are obtained in PIV and UIV, by seeding the flow with tracer particles (or using already present tracers, such as red blood cells) and recording two images of the flow in rapid succession. The displacement of the flow in the time between the two

images is determined in a grid of points, using the local cross correlation of the two images [1,20]. PLIF uses a fluorescent fluid to monitor species concentration in a selected plane in a flow [36], it is often combined with PIV to (simultaneously) measure the velocity field in the same plane. Finally, CDUS is also based on the Doppler frequency shift, but uses phase-shift autocorrelation or time domain correlation, instead of the full Doppler shift information, to obtain real-time velocity information in a number of points in a sub-area of an ultrasound image [8].

Each of these techniques has its own advantages: bulk measurement of flow rate and pressure is relatively simple and affordable to implement both in-vitro and in-vivo, which also holds for ultrasound Doppler techniques. On the other hand, spatial detail and overview can more easily be obtained with whole-field methods, while point measurements, such as LDA, give high accuracy and a high measurement rate more locally. Furthermore, optical techniques such as LDA, PIV and PLIF need optical access, which means that these techniques are not suited for application in-vivo. The point and whole-field methods listed here typically give 2D results, although most of them can be extended to 3D measurements.

Ideally, the experimental techniques to use in a given situation are chosen based on the required flow parameters, accuracy, and spatial and temporal resolution. The experimental set-up can then be designed based on this choice. In practice, also factors such as cost, availability, and ease of implementation and use will play an important role.

2.2 Relevant dimensionless numbers

Dimensionless numbers characterise certain aspects of a flow, which is helpful to obtain a-priori information about this flow. In experimental work, the use of dimensionless numbers is necessary if the experimental geometry is to be scaled with respect to the original geometry, to retain dynamic similarity. In order to be able to draw valid conclusions from an in-vitro experiment, the relevant dimensionless numbers should be matched with those of the flow that is modelled. Once dynamic similarity is attained, also the boundary conditions of the flow should be matched.

An important dimensionless number in nearly every application in fluid dynamics is the Reynolds number [32]:

$$\mathrm{Re} = \frac{\rho U L}{\mu}, \tag{1}$$

with ρ and μ the density and (dynamic) viscosity of the fluid, respectively, and U and L characteristic velocity and length scales. The Reynolds number gives an estimate of the relative importance of inertial and viscous forces in a flow – a low value indicates that viscous forces will be dominant, while a high value means that the flow is likely to be turbulent. For pulsatile flows often a mean and a peak Reynolds number are given, based on the mean and peak flow velocities, respectively. Typical values for the mean Re in vascular access are around 1 000. For straight pipe flow this would imply laminar flow, but the complex geometry of a vascular access site often leads to flow separation and local turbulence, so that the Reynolds number should only be used to achieve dynamic similarity, and not to predict the character of the flow in this case.

To quantify the pressure loss in a flow in relation to the kinetic energy, the Euler number is used:

$$\mathrm{Eu} = \frac{\Delta p}{\rho U^2}, \tag{2}$$

with Δp the pressure drop between two points of interest.

For pulsatile flow, such as encountered in the human body, also transient inertial effects may become important. To assess these effects for (fully developed, rigid) tube flow, the Womersley number [42] is used, commonly denoted by α:

$$\alpha = L\sqrt{\frac{\rho\omega}{\mu}}. \tag{3}$$

Here, ω is the pulsatile flow frequency (in radians/s), and L again a characteristic length scale. It should be noted that generally the tube *radius* is used as a characteristic length scale for the Womersley number, while for the Reynolds number the tube *diameter* is used. A low value of α means that transient inertial forces are relatively unimportant, so that the flow is able to follow the oscillating pressure gradient, and the velocity profile of the flow will be close to a parabolic Poiseuille profile throughout the full cardiac cycle. On the other hand, if α is high, the phase lag of the velocity with respect to the pressure gradient varies considerably across the radius of the tube. As a result, the direction of the flow close to the centreline can be opposite to that close to the wall during part of the cardiac cycle.

Womersley's analysis was originally meant to analyse flow due to an oscillating pressure gradient with negligible mean (e.g. femoral artery of a dog). However, pressure gradient waveforms in vascular access often have a substantial steady component, and the Womersley number as defined above is not sufficient to characterise the flow (see e.g. Kumar et al. [24]). Therefore, we feel it would be better to use an adapted Womersley number in this context, which incorporates the influence of the steady component of the flow, for example by using an amplitude weighted average.

In this context, also the pulsatility index, $u_\mathrm{o}/u_\mathrm{s}$, with u_o the amplitude of the oscillating velocity component, and u_s the steady velocity component, is important to take into account.

Because of the relatively high steady component of a typical vascular access pressure waveform (i.e. low pulsatility index), the velocity profile at the inlet of a vascular access site may be expected to be close to parabolic, which facilitates matching of the inlet boundary condition between computational and experimental work (assuming that both allow for sufficient flow development upstream of the vascular access site).

In addition to the dimensionless numbers listed here, also the Dean number can be useful in the context of vascular access hemodynamics. This number characterises the importance of centrifugal forces in a curved flow geometry, with a high Dean number indicating flow separation. However, for the purpose of dynamic similarity, matching the numbers listed here should be sufficient (Buckingham Pi theorem [7]).

3 Reported applications in vascular access

3.1 Arterio-Venous Fistula

An arterio-venous fistula (AVF) is a connection between an artery and a vein surgically created to deliver increased flow to the vein, thus facilitating dialysis. An AVF is usually located in the arms but can sometimes be made in the legs. Because nowadays an AVF is the preferred modality for vascular access, the majority of the reported work is performed in AVF models.

An early in-vitro study on an idealised radiocephalic AVF was performed by **Sivanesan et al.** [35] in 1999. The goal of this work was to obtain detailed information about the flow structures in an AVF, and the shear stresses related to these. The researchers used particle streak imaging to visualise the flow patterns in two mutually perpendicular planes, which both contained the centreline of the artery. Laser Doppler Anemometry (LDA) was used to measure the axial and radial velocity components along the arterial floor in the anastomosis region, and along several selected lines perpendicular to the centreline of the vein, in the AVF's symmetry plane. The wall shear stresses and turbulent Reynolds shear stresses were derived from these velocity measurements. Both steady and patient-specific pulsatile flow were studied, at (mean) Reynolds numbers of 100 (only steady), 300, and 600. The working fluid for the particle streak imaging was a water-glycerol-sodium chloride mixture with a kinematic viscosity similar to that of blood, while for the LDA measurements, the mixture was adapted to match the refractive index of the silicone rubber that was used for the AVF model.

The observed flow patterns did not significantly differ between steady and pulsatile flow, and also in pulsatile flow the flow patterns did not change significantly throughout the flow cycle. The authors attribute this to the relatively low pulsatility index (pulsatile velocity amplitude/mean velocity) of the applied waveform. The peak wall shear stress measured at the suture line was concluded to be high enough to be potentially damaging to the endothelial cells in the blood vessel wall, although because of the short duration of this peak stress, no firm conclusions could be drawn.

Within the framework of the European Union funded project ARCH [40], **Van Canneyt et al.** [37] performed pressure measurements in a compliant, silicone radio-cephalic AVF model (artery and vein inner diameters: 4 and 7 mm, respectively, 60° angle, see also figure 1) with several degrees of stenosis (25 and 50%) in different positions, to test a novel approach for early stenosis detection. Arterial and venous needles were inserted into the model, and the pressure was measured at the arterial needle and at the inlet of the model (proximal artery). Analysis of the results showed a statistically significant change in the ratio between these two values due to the presence of stenosis, and even the position of the stenosis can be distinguished from this ratio.

In this same project, **Huberts et al.** [17,18] did experiments on an in-vitro test bench to validate flow rates predicted by a lumped parameter, 1D pulse wave propagation model. The test bench consisted of compliant silicone tubes representing the aorta and arm vasculature, in which flow rate and pressure were measured at several positions. Experimentally determined geometrical and mechanical parameters were used as an input for the computational model. The uncertainty for each of these measurements was estimated, and the propagation of these uncer-

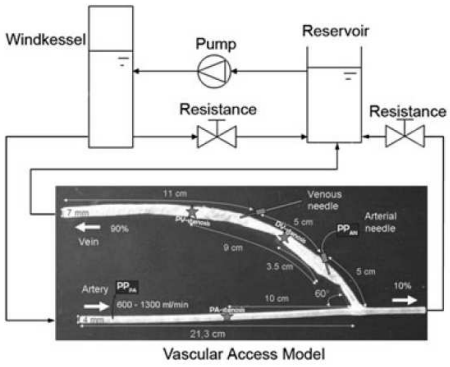

Fig. 1 Vascular access model and flow loop used by Van Canneyt et al. [37]. Dimensions and locations of needles and stenoses are indicated. Reproduced with permission from the author.

tainties through the computational model was studied. It was concluded that the computational model was well able to reproduce the flow rates measured in the experimental set-up, but that uncertainty in the input parameters has a significant influence on the uncertainty of the model results. With an aortic outflow of around 5 l/min as an inlet boundary condition, uncertainties ranging from 5% to 20% in the measured geometrical and mechanical parameters, resulted in uncertainties between 13% and 60% in the simulated mean flow rates. This indicates that it is essential to take measurement uncertainty into account when using experimental results as input for the computational model.

Finally, researchers in this project performed CFD simulations in a patient-specific AVF (reported by **Botti et al.** [4]), and qualitatively verified the results using PIV measurements in a 4:1 scaled model, keeping the Reynolds and Euler numbers constant for dynamic similarity. A refractive index matching water-glycerol mixture was used as a test fluid, and in order to simplify the experimental set-up, steady flow was applied, and the distal artery outlet was occluded. Flow rates corresponding to 220 ml/min and 400 ml/min in the 1:1 geometry were tested. Satisfactory agreement between the CFD and PIV results was found, although the PIV results were more diffusive than the CFD results, due to time averaging (i.e. PIV acts as a temporal filter, leading to a smoothing of the results). Also the pressure drops, measured in the same experimental set-up, showed good agreement with the numerical results, provided that a sufficiently fine mesh was used for the highest flow rates. The measured values fell within one standard deviation from the simulation result. Unfortunately, no quantitative results are reported for the CFD-PIV comparison; the conclusions on this remain restricted to rather vague, qualitative terms.

Combined CFD-PIV studies like the latter are reported fairly often. In 2010, **Kharboutly et al.** [19] carried out computational fluid dynamics (CFD) simulations and PIV measurements in a patient-specific brachio-cephalic AVF model, to validate the numerical simulation method that the authors are using. For the PIV measurements, a rigid, poly-methylmethacrylate (PMMA) model was used, with a 40 vol% aqueous glycerol solution to match the viscosity of blood (4×10^{-3} Pa·s), and a patient-specific waveform applied at the inlet.

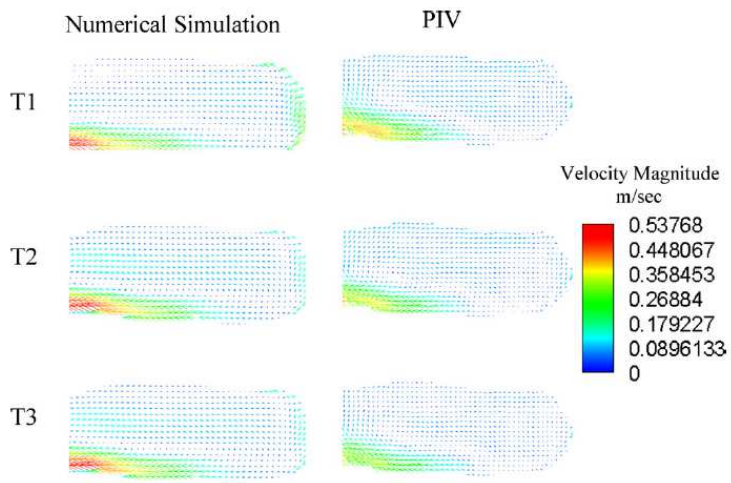

Fig. 2 Comparison of CFD (left column) and PIV (right column) results in the mid-plane of a patient-specific AVF, at different instances during the cardiac cycle. From Kharboutly et al. [19], reproduced with permission from Elsevier.

Remarkably, no refractive index matching or fluorescent seeding particles were used. This suggests that the images of the flow must have suffered from distortion and reflections near the model wall. The authors indeed report a 5% data loss due to these effects.

Velocity vector plots resulting from CFD and PIV were compared qualitatively in two mutually perpendicular planes, at several instances during the cardiac cycle (figure 2). Furthermore, a more quantitative comparison was made by plotting velocity profiles along selected cross-section lines. The average difference between the CFD and PIV results on these lines did not exceed 10%, which is surprisingly good considering the fact that the flow is highly irregular and three-dimensional (out-of-plane motion can significantly degrade the quality of planar PIV measurements).

A similar study was done by researchers from the same group in 2014, to validate numerical simulations of non-Newtonian flow in a compliant, patient specific AVF (reported by **Decorato et al.** [12]). In this case, a rigid, directly 3D-printed PMMA model was used for PIV measurements in a steady, Newtonian flow (water-glycerol mixture, 1.1 l/min). Velocity plots along selected cross-section lines were compared, and the CFD results are reported to fall within the experimental uncertainty of the PIV results (although this is not quite clear from the reported plots). This agreement suggests that the influence of wall compliance and non-Newtonian flow behaviour are negligible in this particular situation, although the authors do not discuss this.

Also researchers in the group of Barber report the use of PIV to validate numerical simulations in an AVF (for example, **Barber et al.** [2] and **Lwin et al.** [27]). Lwin et al. [27] used a mixture of water, glycerol and sodium iodide (NaI) to match the refractive index of their test fluid with that of the PMMA flow phantom. Vector plots and velocity profiles in the mid-plane of an AVF were compared under steady flow conditions. The PIV velocity profiles are reported to agree with the

CFD results, although the PIV results fail to capture a high-velocity peak in the profile. The authors tentatively attribute this to a too large time interval between the captured particle images, and indicate that further research is necessary to find the source of this discrepancy.

Another example of the use of bulk parameter measurements to validate computational work, is the paper by **Browne et al.** [6]. The authors use an idealised, representative model of an AVF to record the pressure signal at several different positions, at different steady flow rates. The measured pressure drops agree well with the computed ones, staying within roughly one standard deviation of the CFD results, indicating that the computational model is capable of capturing the complex dynamics of the flow.

Table 2 Geometries of AVF experiments reviewed (in order of discussion).

Paper	Geometry	Stiffness
Sivanesan et al. [35]	Idealised	Rigid
Van Canneyt et al. [37]	Idealised, based on patient data	Compliant
Huberts et al. [17,18]	Idealised, based on patient data	Compliant
Botti et al. [4]	Patient-specific	-
Kharboutly et al. [19]	Patient-specific	Rigid
Decorato et al. [12]	Patient-specific	Rigid
Barber et al. [2]	-	Rigid
Lwin et al. [27]	Idealised	Rigid
Browne et al. [6]	Idealised	Rigid

- Data not available

Table 3 Hemodynamic conditions of AVF experiments reviewed (in order of discussion).

Paper	Liquid	Re	Flow Rate (ml/min)
[35]	Water-glycerol-NaCl (40-46-14%)	100, 300, 600	-
[37]	Water-glycerol (62-38%)	-	500-1300
[17,18]	Water	-	5000
[4]	Water-glycerol	550, 1000	220, 400
[19]	Water-glycerol (60-40%)	-	1840, 2000, 2450
[12]	Water-glycerol (70-30%)	-	1000
[2]	-	-	-
[27]	NaI, water, glycerol (53-30-16.3%)	-	780, 1200
[6]	Water-glycerol (65-35%)	-	-

- Data not available

3.2 Arterio-Venous Graft

An arterio-venous graft (AVG) is a connection between an artery and a vein via a graft. Grafts are usually constructed from synthetic materials but can also be made from biological materials. Similar to an AVF, AVGs are generally placed in the upper limbs and can also be positioned in the lower limbs. The use of experimental

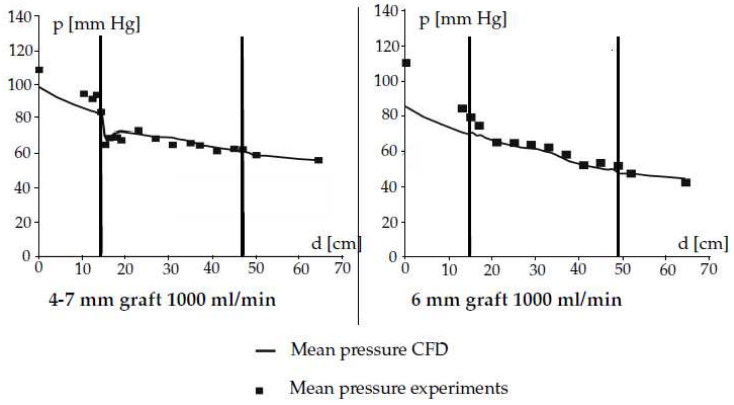

Fig. 3 Comparison of CFD results (solid line) with in-vitro pressure measurements (square markers) in a tapered (left) and a straight (right) graft. The arterial inlet is located at $d = 0$ cm, the arterial anastomosis at $d = 15$ cm, the venous anastomosis at $d = 49$ cm, and the venous outlet at $d = 69$ cm. From Van Tricht [38] (chapter 5), reproduced with permission.

modelling to verify a computational model is also seen in the case of AVGs [38, 11, 10, 26]. However, in this case experimental modelling is also used as a tool on its own [15, 39, 38, 22, 21].

Heise et al. [15] use PIV measurements in transparent Silastic models to compare the flow velocity and vorticity fields in AVGs with a straight and a cuffed anastomosis. A pulsatile inlet flow is applied, and the test fluid is a mixture of water and glycerol that matches the viscosity of blood. The authors do not mention the use of refractive index matching, but the refractive index of the water-glycerol mixture is expected to be close to that of Silastic (a silicone rubber type by Dow Corning). The recording of the particle images was synchronised with the pulsatile flow, and for each time point in the flow cycle the average of 5 measurements was used to increase the accuracy of the results. Vector plots of the velocity and vorticity are given, together with plots of the variation of velocity and shear stress over time in several different points. The results show differences in vorticity and shear stress patterns between the two types of graft, with the cuffed graft resulting in a more homogeneous distribution of shear stress and vorticity.

Also **Van Tricht et al.** [39] compared two different types of AVG. The authors monitored flow rate and pressure in compliant silicone tubes connected with either a straight or a tapered loop graft, using a water-glycerol mixture as a Newtonian blood analogue. Apart from a higher pressure drop at the arterial anastomosis of the tapered graft, no significant differences between the two graft types were found.

Later on, these experimental results were used by Van Tricht [38] (chapter 5) to validate and provide boundary conditions for numerical simulations in the same geometries. Rigid walls were assumed in the simulations and, even though the CFD results underestimate the pressure drop at some locations, the values between the arterial and venous anastomosis are captured well (figure 3).

In the same thesis (chapter 8), Van Tricht describes experiments to study the effects of the presence of needles on the flow during a hemodialysis session. The experimental set-up consists of a flow loop through the silicone vascular access

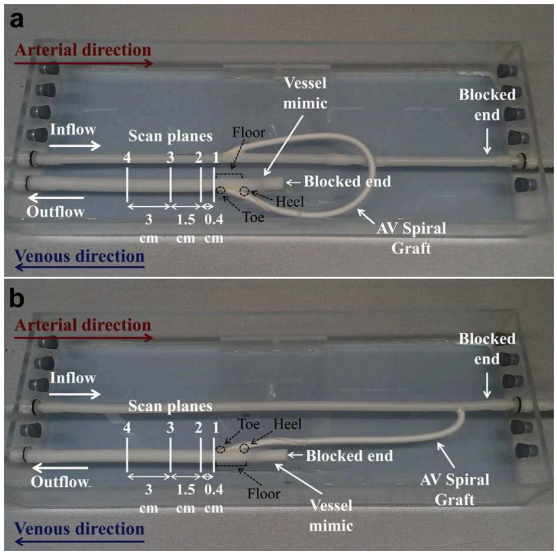

Fig. 4 Experimental set-up used by Kokkalis et al. [21], a) looped configuration, b) straight configuration. Reproduced with permission from Elsevier.

model, with a flow loop representing the dialysis machine connected to it through an arterial and a vascular needle. A water-glycerol test fluid was used, and a representative pulsatile flow waveform was applied at the arterial inlet of the model. Pressure and velocity signals were recorded at several locations, for different flow rates in both flow loops. It was concluded that the flow rate of the hemodialysis machine should be carefully adjusted to that in the vascular access vein, to prevent hypertension, recirculation and high wall shear rates.

Another example of experimental modelling being used on its own is the work by **Kokkalis et al.** [22,21]. These papers describe ultrasound Vector Doppler experiments in an in-vitro set-up, to verify the assumption of helical flow induced by a novel type of AVG. The novel spiral flow inducing graft and a reference graft were tested in a looped and a straight configuration (figure 4), under steady flow conditions. The velocity field in four cross-sectional planes downstream of the graft was reconstructed from Vector Doppler measurements in a number of points across the plane. Additionally, also Colour Doppler recordings were made. In both configurations, the spiral graft was observed to lead to a higher in-plane velocity and circulation in the measurement planes (figure 5), suggesting increased in-plane mixing, which is believed to be beneficial for the vein.

Finally, in the papers by **Chen et al.** [11,10], and **Lin et al.** [26], the cardiovascular system is modelled as an electrical circuit (figure 6). The idea behind this is that flow instabilities induced by an artificially created vascular access induce vibrations in the elastic vessel wall, and that the flow resistance and vessel compliance affect the rise time, amplitude and time interval of the transverse vibration pressure associated with these vessel wall vibrations. The vascular access is represented by a lumped resistor, R, and a lumped capacitance, C, with time constant $\tau = R \times C$. Stenosis would result in high resistance and low compliance, influencing the blood pressure signal, and hence the value of τ. In case τ becomes

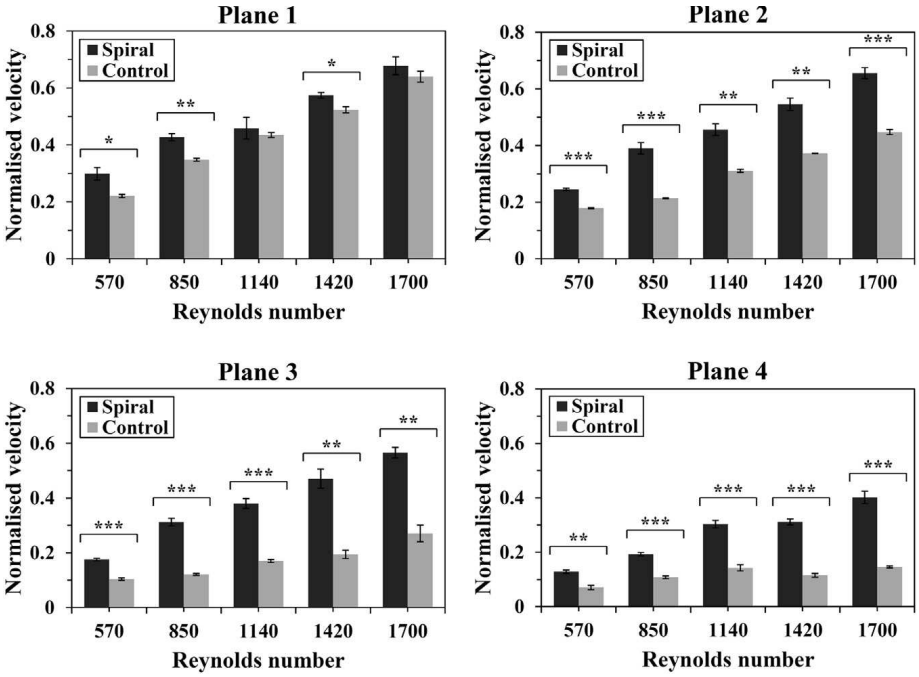

Fig. 5 Measured peak in-plane velocity in scan planes 1 to 4 downstream of the outflow of the spiral and control straight grafts as a function of the applied Reynolds number. * $p \leq 0.05$, ** $p \leq 0.01$, *** $p \leq 0.001$. From Kokkalis et al. [21], reproduced with permission from Elsevier.

negative, the pole of the equivalent electrical circuit becomes positive, and the system's response becomes unstable. This model was validated experimentally by measuring pressure signals in different locations in an in-vitro set-up representing the relevant vasculature for AV access with an AVG. Different degrees of stenosis, varying from 50 to 95%, were studied in the experiments. A water-glycerol mixture was used as a test fluid, and representative pulsatile flow was applied. Pressure was monitored using venous needles and static pressure transducers. The time constant, τ, obtained from the measured pressure signal, was indeed shown to correlate positively (linear regression with $R^2 = 0.87$) with the degree of stenosis.

Table 4 Geometry of AVG experiments reviewed (in order of discussion).

Paper	Geometry	Material
Heise et al. [15]	Straight and Cuffed	PTFE
Van Tricht et al. [39]	Straight and Tapered	PTFE
Van Tricht [38]	Straight	PTFE
Kokkalis et al. [22,21]	Straight and Spiral	ePTFE
Chen et al. [11,10]	Electrical Circuit	Silcone Tubes
Lin et al. [26]	-	-

- Data not available

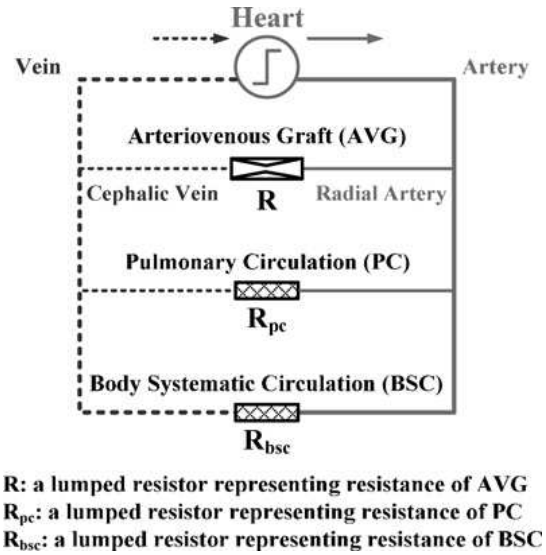

Fig. 6 Electrical circuit representing the cardiovascular system of a hemodialysis patient. From Chen et al. [11], reproduced by permission of the Institution of Engineering & Technology.

Table 5 Hemodynamic conditions of AVG experiments reviewed (in order of discussion).

Paper	Liquid	Re	Flow Rate (ml/min)
[15]	Water-glycerol (58-42%)	-	500
[39]	Water-glycerol (60-40%)	933, 2800	500-1500
[38]	Water-glycerol (60-40%)	-	500, 1000, 1500
[22,21]	Water-glycerol (91-9%)	570, 850, 1140, 1420, 1700	240, 360, 480, 600, 720
[11,10]	Water-glycerol	-	600-1000
[26]	-	-	-

- Data not available

3.3 Central Venous Catheter

A central venous catheter (CVC) is a flexible tube used to provide dialysis. It is commonly inserted into a vein in the chest, neck or groin. Literature on experimental modelling in research on CVCs is rather limited. One example is the paper by **Mareels et al.** [28], in which PIV is used to validate CFD studies of three different CVC geometries. Transparent silicone models, scaled up by a factor of 2.8, were used for the experimental set-up. To minimise distortions due to refraction, the superior vena cava (SVC) was modelled by a rectangular duct. Because the study focuses on the outflow of the CVC, with the SVC walls relatively far away, the modified SVC geometry is not expected to significantly influence the results. A refractive index matching water-glycerol mixture was used as a test fluid, at a temperature of 50 °C to match the viscosity of blood. Fluorescent tracer particles were used, in combination with a band-pass filter on the camera lens, to block reflections. Steady flow was applied, and measurements were taken in two mutually perpendicular planes. The CFD and PIV results were compared qualitatively by

means of velocity magnitude color plots, and the velocity magnitude was averaged over the entire plane for quantitative comparison. Relative errors of up to 34% were found, which the authors tentatively attribute to small differences between the PIV and CFD measurement planes.

The last paper to be discussed in this review is one by **Barbour et al.** [3]. Instead of focusing on wall shear stress, the experiments described in this paper aim to assess the effectiveness of the heparin locking procedure that is routinely applied in CVCs that are not in use. This procedure comprises filling a CVC with the anti-coagulant heparin while not in use, to maintain patency and prevent thrombus formation at the catheter tip. For the experiments a CVC was filled with a rhodamine-B dye that acted as a heparin mimic. This was inserted into a model SVC, a straight, acrylic pipe, which was enclosed by a rectangular box filled with the same water-glycerol mixture that was used for the flow in the pipe, to minimise distortions due to refraction. A representative pulsatile waveform was applied at the inlet, and fully developed flow was ensured at the entrance of the test section. The velocity field was measured using PIV, while the heparin concentration was monitored by Planar Laser Induced Fluorescence (PLIF), both in pulsatile flow and quiescent conditions. The results are consistent with previous in-vivo estimates of 24-hour leakage rates, and show that the pulsatile flow around the catheter drives a convection-diffusion process, which rapidly depletes the heparin concentration in the near-tip region of the catheter.

Table 6 Geometry of CVC experiments reviewed (in order of discussion).

Paper	Geometry	Material
Mareels et al. [28]	Step-tip catheter	Silicone
Barbour et al. [3]	Split-tip catheter	-

- Data not available

Table 7 Hemodynamic conditions of CVC experiments reviewed

Paper	Liquid	Re	Flow Rate (ml/min)
[28]	Water-glycerol (42-58%)	937	784
[3]	Water-glycerol (60-40%)	1050	30 ml stroke volume at 54 BPM

4 Discussion, conclusions and recommendations

Experimental modelling is frequently employed to study different aspects of the hemodynamics in an in-vitro vascular access model, either to support computational modelling work, or as a tool on its own. The experimental methods that are used (see also table 1) are mostly well-established, their worth proven in other fields of fluid mechanics.

Newtonian water-glycerol mixtures of varying composition are used as a blood mimic in most applications, aiming to match the dynamic viscosity, μ, of blood. Considering the predominant focus on wall shear stress, this is a logical choice.

However, in view of the apparent importance of flow instabilities and turbulence in vascular access, matching the kinematic viscosity, $\nu = \mu/\rho$, may be a better option, as this faciliates matching the Reynolds and Womersley numbers.

In cases where optical access is required, popular transparent materials are silicone rubbers and acrylic plastics. In some cases the use of glycerol and/or sodium iodide in the test fluid is reported, to achieve refractive index matching between the test fluid and the flow phantom material.

Since the use of shear stress sensors (e.g. Horowitz et al. [16]) is highly impractical in in-vitro hemodynamics experiments, and the use of pressure drop measurements to determine the wall shear stress implies averaging over a certain section, local wall shear stress values are usually determined from an estimate of the wall shear rate. When a Newtonian test fluid is used, shear stress is directly proportional to shear rate, with μ the proportionality constant. The wall shear rate is obtained by either assuming a certain velocity profile and computing its derivative, or by estimating the slope of the actual velocity profile at the wall from a few measurement points close to the wall. This makes these wall shear stress estimates sensitive to measurement errors (see also e.g. Ku [23]). Consequently, it should be realised that wall shear stress is not the most suitable parameter for validation purposes.

Apart from a few exceptions (e.g. [18]), the studies discussed in this review do not go into detail on the accuracy and uncertainty of the used experimental methods. Papers that use experimental modelling to validate computational work generally do not elaborate on the criteria used to accept or reject their computational model.

To increase the practical impact of computational models, a more rigorous verification and validation procedure should be adopted (see also, for example, the work of Oberkampf and co-workers [30,34]). As mentioned in the introduction, in the context of computational fluid dynamics the term verification is generally used for the process of ascertaining that the discretised equations converge to the original analytical model equations (e.g. discretisation error estimation, mesh convergence), while the term validation is used to indicate testing whether the model, with all its assumptions, realistically represents the modelled process, within the intended range of parameter values.

In the context of hemodynamics modelling in vascular access, we propose to use a two-step validation process. First, it should be ascertained that the computational model correctly represents the conceptual model (e.g. does the computational model correctly represent Newtonian flow in a rigid vessel under the applied conditions?). As stated in the introduction (1), experimental modelling is particularly useful for this step, because of the high accuracy and reproducibility that can be achieved with an in-vitro set-up.

The next step is to validate the model *assumptions*, that is, to assess whether the model sufficiently accurately captures the key features of the process that it was intended to represent (e.g. does a model assuming Newtonian flow in a rigid vessel realistically represent the hemodynamics in AV access?). For this step in-vivo measurements are necessary, and parameters that can be readily extracted from the simulation results and in-vivo measurements should be selected. The accuracy and uncertainty of the applied measurement method, and the reproducibility and variability of the required experiments should be carefully considered. In-vitro experimental modelling can be instrumental in the quantification of the accuracy,

uncertainty, and reproducibility of a measurement method, before it is applied in-vivo.

Interesting emerging methods for detailed in-vivo validation of CFD are, for example, Ultrasound Imaging Velocimetry (UIV) [31,25] and 4D Flow MRI [29]. Both methods are capable of measuring whole velocity fields with a high spatial resolution, comparable to PIV, but without the need for optical access. The main advantage of UIV over 4D Flow MRI is that it takes relatively little time to complete a measurement. In case of vascular access, an additional advantage is that vessels in the arm can be more easily accessed by an ultrasound probe than by MRI. On the other hand, 4D Flow MRI inherently gives three-dimensional results, whereas to achieve this with UIV, multiple measurements and extra post-processing are required.

Finally, it should be noted that methods like CFD, PIV, UIV, and 4D Flow MRI are especially suitable to increase the understanding of the role of hemodynamics in vascular access failure. However, for day-to-day use in clinical practice, for example, for the prediction and detection of stenosis, simpler measurement methods and computational models are generally preferred. The challenge is to use the knowledge obtained from the more involved studies to improve the simpler tools, and to derive guidelines for clinical practice.

Acknowledgements This project has received funding from the European Unions Seventh Framework Programme for research, technological development and demonstration under grant agreement no. 324487.

References

1. Adrian, R.J., Westerweel, J.: Particle Image Velocimetry, *Cambridge Aerospace Series*, vol. 30. Cambridge University Press (2011)
2. Barber, T., Fulker, D., Lwin, N.M., Simmons, A.: Using fluid dynamics to improve vascular access in haemodialysis. Renal Society of Australasia Journal **11**(1), 32–34 (2014)
3. Barbour, M.C., McGah, P.M., Ng, C.H., Clark, A., Gow, K.W., , Aliseda, A.: Convective leakage makes heparin locking of central venous catheters ineffective within seconds: experimental measurements in a model superior vena cava. ASAIO Journal **61**(6), 701–709 (2015)
4. Botti, L., Van Canneyt, K., Kaminsky, R., Claessens, T., Planken, R.N., Verdonck, P., Remuzzi, A., Antiga, L.: Numerical evaluation and experimental validation of pressure drops across a patient-specific model of vascular access for hemodialysis. Cardiovascular Engineering and Technology **4**(4), 485–499 (2013)
5. Browne, L.D., Bashar, K., Griffin, P., Kavanagh, E.G., Walsh, S.R., Walsh, M.T.: The role of shear stress in arteriovenous fistula maturation and failure: a systematic review. PLOS-One (2015). DOI 10.1371/journal.pone.0145795
6. Browne, L.D., Walsh, M.T., Griffin, P.: Experimental and numerical analysis of the bulk flow parameters within an arteriovenous fistula. Cardiovascular Engineering and Technology **6**(4), 450–462 (2015)
7. Buckingham, E.: On physically similar systems; illustrations of the use of dimensional equations. Physical Review **IV**(4), 345–376 (1914)
8. Bushberg, J.T., Seibert, J.A., Jr., E.M.L., Boone, J.M.: The Essential Physics of Medical Imaging. Wolters Kluwer Health, Lippincott Williams & Wilkins, Philadelphia (2012)
9. Caroli, A., Manini, S., Antiga, L., Passera, K., Ene-Iordache, B., Rota, S., Remuzzi, G., Bode, A., Leermakers, J., van de Vosse, F.N., Vanholder, R., Malovrh, M., Tordoir, J., Remuzzi, A.: Validation of a patient-specific hemodynamic computational model for surgical planning of vascular access in hemodialysis patients. Kidney International **84**, 12371245 (2013)

10. Chen, W.L., Kan, C.D., Kao, R.H.: Numerical evaluation and experimental validation of vascular access stenosis estimation. Technology and Healthcare **24**(s1), S245–S252 (2015)
11. Chen, W.L., Lin, Y.H., Kan, C.D., Yu, F.M., Lin, C.H.: Assessment of flow instabilities in in-vitro stenotic arteriovenous grafts using an equivalent astable multivibrator. IET Science, Measurement & Technology **9**(6), 709–716 (2015)
12. Decorato, I., Kharboutly, Z., Vassallo, T., Penrose, J., Legallais, C., Salsac, A.V.: Numerical simulation of the fluid structure interactions in a compliant patient-specific arteriovenous fistula. International Journal for Computational Methods in Biomedical Engineering **30**, 143–159 (2014)
13. Dixon, B.S.: Why don't fistulas mature? Kidney International **70**, 1413–1422 (2006)
14. Dunmire, B., Beach, K.W., Labs, K.H., Plett, M., Jr., D.E.S.: Cross-beam vector Doppler ultrasound for angle-independent velocity measurements. Ultrasound in Medicine and Biology **26**(8), 1213–1235 (2000)
15. Heise, M., Schmidt, S., Krüger, U., Pfitzmann, R., Scholz, H., Neuhaus, P., Settmacher, U.: Local haemodynamics and shear stress in cuffed and straight PTFE-venous anastomoses: an in-vitro comparison using Particle Image Velocimetry. European Journal of Vascular and Endovascular Surgery **26**, 367–373 (2003)
16. Horowitz, S., Chen, T., Chandrasekaran, V., Tedjojuwono, K., Nishida, T., Cattafesta, L., Sheplak, M.: A micromachined geometric Moiré interferometric floating-element shear stress sensor. In: 42nd AIAA Aerospace Sciences Meeting and Exhibit (2004)
17. Huberts, W., Bode, A., Kroon, W., Planken, R., Tordoir, J., van de Vosse, F., Bosboom, E.: A pulse wave propagation model to support decision-making in vascular access planning in the clinic. Medical Engineering & Physics **34**(2), 233–248 (2011)
18. Huberts, W., Van Canneyt, K., Segers, P., Eloot, S., Tordoir, J., Verdonck, P., van de Vosse, F., Bosboom, E.: Experimental validation of a pulse wave propagation model for predicting hemodynamics after vascular access surgery. Journal of Biomechanics **45**, 1684–1691 (2012)
19. Kharboutly, Z., Deplano, V., Bertrand, E., Legallais, C.: Numerical and experimental study of blood flow through a patient-specific arteriovenous fistula used for hemodialysis. Medical Engineering & Physics **32**, 111–118 (2010)
20. Kim, H.B., Hertzberg, J.R., Shandas, R.: Development and validation of echo-PIV. Experiments in Fluids **36**, 455–462 (2004)
21. Kokkalis, E., Cookson, A.N., Stonebridge, P.A., Corner, G.A., Houston, J.G., Hoskins, P.R.: Comparison of vortical structures induced by arteriovenous grafts using vector Doppler ultrasound. Ultrasound in Medicine and Biology **41**(3), 760–774 (2015)
22. Kokkalis, E., Hoskins, P.R., Corner, G.A., Stonebridge, P.A., Doull, A.J., Houston, J.G.: Secondary flow in peripheral vascular prosthetic grafts using vector Doppler imaging. Ultrasound in Medicine and Biology **39**(12), 2295–2307 (2013)
23. Ku, D.N.: Blood flow in arteries. Annual Review of Fluid Mechanics **29**, 399434 (1997)
24. Kumar, L., Mehandia, V., Narayanan, S.: Modeling laminar pulsatile flow for superior cleaning of fouling layers. Industrial & Engineering Chemistry Research **54**, 10,89310,900 (2015)
25. Leow, C.H., Bazigou, E., Eckersley, R.J., Yu, A.C.H., Weinberg, P.D., Tang, M.X.: Flow velocity mapping using contrast enhanced high-frame-rate plane wave ultrasound and image tracking: methods and initial in vitro and in vivo evaluation. Ultrasound in Medicine and Biology **41**(11), 2913–2925 (2015)
26. Lin, C.H., Dann, C.D., Chen, W.L., Wu, M.J., Yu, F.M.: An equivalent astable multivibrator model to assess flow instability and dysfunction risk in in-vitro stenotic arteriovenous grafts. Technology and Health Care **24**(3), 295–308 (2016)
27. Lwin, N., Wahab, M., Carroll, J., Barber, T.: Experimental and computational analysis of a typical Arterio-Venous Fistula. In: 19th Australasian Fluid Mechanics Conference (December, 2014)
28. Mareels, G., Kaminsky, R., Eloot, S., Verdonck, P.R.: Particle Image Velocimetryvalidated, computational fluid dynamicsbased design to reduce shear stress and residence time in central venous hemodialysis catheters. ASAIO Journal **53**, 438446 (2007)
29. Markl, M., Frydrychowicz, A., Kozerke, S., Hope, M., Wieben, O.: 4d flow MRI. Journal of Magnetic Resonance Imaging **36**, 1015–1036 (2012)
30. Oberkampf, W.L., Trucano, T.G.: Verification and validation in computational fluid dynamics. Progress in Aerospace Sciences **38**, 209–272 (2002)
31. Poelma, C., van der Mijle, R., Mari, J., Tang, M.X., Weinberg, P., Westerweel, J.: Ultrasound imaging velocimetry: Toward reliable wall shear stress measurements. European Journal of Mechanics B/Fluids **35**, 70–75 (2012)

32. Reynolds, O.: An experimental investigation of the circumstances which determine whether the motion of water shall be direct or sinuous, and of the law of resistance in parallel channels. Philosophical Transactions of the Royal Society **174**, 935–982 (1883)
33. Rothuizen, T.C., Wong, C.Y., Quax, P.H.A., van Zonneveld, A.J., Rabelink, T.J., Rotmans, J.I.: Arteriovenous access failure: more than just intimal hyperplasia? Nephrology Dialysis Transplantation **28**, 1085–1092 (2013)
34. Roy, C.J., Oberkampf, W.L.: A comprehensive framework for verification, validation, and uncertainty quantification in scientific computing. Computational Methods in Applied Mechanical Engineering **200**, 21312144 (2011)
35. Sivanesan, S., How, T., Black, R., Bakran, A.: Flow patterns in the radiocephalic arteriovenous fisstula: an in vitro study. Journal of Biomechanics **32**, 915–925 (1999)
36. Tropea, C., Yarin, A., Foss, J.F. (eds.): Springer Handbook of Experimental Fluid Mechanics. Springer (2007)
37. Van Canneyt, K., Planken, R.N., Eloot, S., Segers, P., Verdonck, P.: Experimental study of a new method for early detection of vascular access stenoses: pulse pressure analysis at hemodialysis needle. Artificial Organs **34**(2), 113–117 (2010)
38. Van Tricht, I.: Hemodynamics of vascular access for hemodialysis. Ph.D. thesis, Universiteit Gent (2005)
39. Van Tricht, I., De Wachter, D., Tordoir, J., Verdonck, P.: Hemodynamics in a compliant hydraulic in vitro model of straight versus tapered PTFE Arteriovenous Graft. Journal of Surgical Research **116**, 297–304 (2004)
40. Website: European commission: Community research and development information service. `http://cordis.europa.eu/project/rcn/86679_en.html` (2016). Accessed: June, 2016
41. Website: Homepage: Redva. `http://www.redva.eu` (2016). Accessed: June, 2016
42. Womersley, J.R.: Method for the calculation of velocity, rate of flow and viscous drag in arteries when the pressure gradient is known. Journal of Physiology **127**(3), 553–563 (1955)